Stability, Homodimerization, and Calcium-Binding Properties of a Single, Variant $\beta\gamma$-Crystallin Domain of the Protein Absent in Melanoma 1 (AIM1)†

Bheemreddy Rajini,‡ Caroline Graham,§,|| Graeme Wistow,§ and Yogendra Sharma*,‡

Centre for Cellular and Molecular Biology, Uppal Road, Hyderabad-500007, India, and Section on Molecular Structure and Function, National Eye Institute, NIH, Bethesda, Maryland 20892

Received December 19, 2002; Revised Manuscript Received February 4, 2003

ABSTRACT: AIM1 (absent in melanoma), a candidate suppressor of malignancy in melanoma, is a nonlens member of the $\beta\gamma$-crystallin superfamily, which contains six predicted $\beta\gamma$ domains. The first $\beta\gamma$-crystallin domain of AIM1 (AIM1-g1) diverges most in sequence from the superfamily consensus. To examine its ability to fold and behave like a normal $\beta\gamma$ domain, we cloned AIM1-g1 and overexpressed it in *Escherichia coli* as a recombinant protein. The recombinant domain was found to be a stable, soluble protein, similar to lens protein γB-crystallin in secondary structure. The tertiary structure of AIM1-g1 is dominated by the contribution of aromatic amino acids and cysteine. AIM1-g1 undergoes concentration-independent, noncovalent homodimerization with no trace of monomer, similar to a one-domain protein spherulin 3a. Since many $\beta\gamma$ domain proteins bind calcium, we have also investigated the calcium-binding properties of AIM1-g1 by various methods. AIM1-g1 binds the calcium-mimic dye Stains-all, the calcium probe terbium (with K_D 170 μM), and ^{45}Ca when blotted on a membrane. AIM1-g1 binds calcium (K_D 30 μM) with a comparatively higher affinity than bovine lens γ-crystallin (90 μM). However, calcium binding does not induce significant change in the protein conformation in the near- and far-UV CD and in fluorescence. The AIM1-g1 domain is as stable as domains of $\beta\gamma$-crystallins (βB2- or γS-crystallins) as monitored by guanidinium chloride unfolding (midpoint of unfolding transition is 1.8 M GdmCl), and the stability of the protein is not altered upon binding calcium as evaluated by equilibrium unfolding. These results show that, despite the sequence variation, AIM1-g1 folds such as a $\beta\gamma$ domain, binds calcium and undergoes dimerization.

Absent in melanoma 1 (AIM1)[1] was originally identified as a gene whose expression is associated with suppression of malignancy in melanoma (*1*). AIM1 is expressed in many normal tissues, including skin, liver, lung, heart, and kidney (*2*). It is absent in melanoma cells but is expressed in suppressed melanoma cell lines that have been transfected with the tumor suppressor region of human chromosome 6q21 (*1*, *3*).

Structurally, AIM1 belongs to the $\beta\gamma$-crystallin superfamily (*1*). This is an ancient and diverse superfamily represented by proteins expressed in many species, ranging from prokaryotes to mammals. These proteins share structural similarity with the related β- and γ-crystallins of the vertebrate eye lens (*4*). This is reflected by the presence of a characteristic Greek key motif of about 40 residues, a supersecondary element that folds into four antiparallel β-strands (a, b, c, and d) (*5*, *6*) and bears a sequence signature that includes structurally important conserved aromatics at positions 5 and 11, glycine at position 13, and serine at position 34, as numbered relative to the first motif of γB-crystallin (*4*, *6*−*9*). Two Greek key $\beta\gamma$ motifs associate with pseudosymmetry to form one domain, and the protein superfamily contains members with one, two, or multiple domains. The lens β- and γ-crystallins (*10*), spore coat protein S from *Myxococcus xanthus* (*11*, *12*), epidermal-differentiation protein EP37 from a Japanese newt (*11*, *13*, *14*), and calcium dependent calmodulin-binding membrane proteins from *Paramecium tetraurelia* (*15*) are some examples of known or predicted two-domain proteins. The one-domain members are represented by spherulin 3a from *Physarum polycephalum* (*16*, *17*), and possibly, by more divergent proteins, WmKT (a toxin) from *Williopsis marakii* (*17*, *18*) and SMPI, a metalloproteinase inhibitor from *Streptomyces* (*19*).

AIM1 is a multidomain nonlens member of the superfamily, with six predicted $\beta\gamma$ domains formed from 12 $\beta\gamma$ Greek key motifs (*1*). In the AIM1 gene, the 12 $\beta\gamma$ motifs are encoded by separate exons with exactly the same intron positions as in the lens β-crystallins. The 12 AIM1 $\beta\gamma$ motifs follow the repeated ABAB pattern with the highest conservation of B-type motifs. However, some A-type motifs are quite

† Supported from the ICMR Grant (IRIS ID #2000-01320). B.R. was supported from the CSIR, India as senior research fellowship.

* Corresponding author. E-mail: yogendra@ccmb.res.in. Fax: +91-402-716-0311. Phone: +91-402-719-2552.

‡ Centre for Cellular and Molecular Biology.

§ National Eye Institute.

|| Current address: NCI/DBS/EIB, National Institute of Health, Bethesda MD 20892.

[1] Abbreviations: AIM1, absent in melanoma 1; AIM1-g1, first $\beta\gamma$ motif of AIM1; DTT, dithiothreitol; Stains-all, 1-ethyl-2-[3-(1-ethylnaphtho[1,2-D]thiazolin-2-ylidene)-2-methylpropenyl]naphtha [1,2-D]-thiazolium bromide; CD, circular dichroism; GdmCl, guanidinium chloride.

10.1021/bi027384l CCC: $25.00
Published on Web 03/27/2003

divergent. The most divergent pair of motifs in AIM1 makes up the first predicted $\beta\gamma$ domain (AIM1-g1). In the first motif of AIM1-g1 some of the key signature residues, particularly the highly conserved Gly13, are replaced by glutamate, and Ser34 is substituted by leucine, while the second motif has an unusually long loop between strands c and d (*1*). However, other features of the sequence are still consistent with the formation of a $\beta\gamma$-like domain. This AIM1-g1 domain helps to explore the limits of relationship between structure and sequence in this superfamily.

While many aspects of the function of $\beta\gamma$-crystallin superfamily proteins are still unclear, several members share the ability to bind calcium ions. In particular, two microbial members of the $\beta\gamma$ superfamily, protein S (*12*, *20*, *21*) and spherulin 3a (*8*, *22*), have been shown to possess calcium-binding sites that have been precisely defined in structural studies. We have earlier demonstrated evidence for calcium binding to bovine lens β_H- and γ-crystallins (*23*−*26*). In this work we have, therefore, cloned and expressed the first $\beta\gamma$ domain of AIM1 (AIM1-g1) and examined the secondary structure, calcium-binding properties, homodimerization, and stability of this single domain. We show that despite its variant cDNA sequence, AIM1-g1 forms a stable, soluble protein with all the characteristics of a $\beta\gamma$ domain, including homodimerization. Furthermore, we show that AIM1-g1 binds calcium, and this property may be relevant to the possible role of AIM1 in the cancerous and normal cell.

EXPERIMENTAL PROCEDURES

Construction and Cloning of the First $\beta\gamma$-Crystallin Domain (AIM1-g1) of AIM1. The sequence and the cloning strategy of the full-length gene of AIM1 have been described earlier (*1*). For subcloning the first two Greek key $\beta\gamma$ motifs (a1 and a2, 96 residues) forming one crystallin domain of AIM1, corresponding to 1021−1117 residues (accession number U83115), gene-specific primers were designed with NdeI and SacI sites and were PCR-amplified. The resultant PCR product was subcloned into a pET17b expression vector (Novagen). The sequence of the clone was confirmed by DNA sequencing on an automated DNA sequencer (ABI Prism 3700). The pET17b-AIM1-g1 clone was transformed into BL21(DE3)plysS cells for protein expression.

Overexpression and Purification of AIM1-g1 Domain. A 1-L culture of *Escherichia coli* BL21(DE3)plysS harboring the appropriate plasmid was grown at 37 °C in 2YT medium supplemented with 100 μg/mL ampicillin to an OD_{600} of 0.6. Protein expression was then induced with 1 mM IPTG. After 4 h of IPTG induction, cells were harvested by centrifugation and lysed by sonication at 4 °C in 50 mM Tris-HCl, pH 8 buffer containing 1 mM EDTA, 100 mM NaCl, and 0.1 mM phenyl methyl sulfonyl fluoride. The lysate was centrifuged at 15 000 rpm for 30 min at 4 °C. The resultant supernatant was then dialyzed against 25 mM Tris-HCl, pH 8, 1 mM EDTA, and 1 mM DTT (buffer A) and applied to a Q-Sepharose fast flow (Pharmacia-Amersham) column pre-equilibrated with buffer A. Protein was eluted using a linear gradient from 0 to 0.5 M sodium chloride in buffer A. The fractions containing AIM1-g1 were pooled, concentrated by an Amicon concentrator, and finally purified on a Superdex 75 (HR 10/30) size-exclusion column (Pharmacia) in buffer A where AIM1-g1 eluted at 12.6 mL.

Far- and Near-UV CD. Circular dichroism (CD) spectra were recorded on a Jasco J-715 spectropolarimeter at room temperature. Far-UV CD of protein was performed in 50 mM Tris-HCl, pH 7, containing 100 mM KCl and 1 mM DTT. The path length used was 0.02 cm, and protein concentration of 1 mg/mL was used. Near-UV CD was performed in the same buffer in a 1 cm path length cell. Protein concentration used for near-UV CD was 0.4 mg/mL. All spectra were baseline corrected. Ellipticities are expressed in millidegrees. The effect of cation on near- and far-UV CD was studied by titrating the protein solution with calcium.

Fluorescence Spectroscopy. Fluorescence emission spectra were recorded in correct spectrum mode on a F-4500 Hitachi Fluorescence spectrophotometer at an excitation wavelength of 295 nm. The excitation and emission band-passes were set at 5 nm each. The effect of calcium on the emission spectra was studied by titrating the protein solution with calcium.

Superdex 75 FPLC. The molecular mass of the protein under native conditions was determined by a properly calibrated Superdex 75 (HR 10/30) size-exclusion column (Pharmacia-Amersham) in 50 mM Tris-HCl, pH 7.2, 100 mM NaCl, 1 mM EDTA, and 3 mM DTT. The flow rate used was 0.5 mL per min.

Equilibrium Unfolding Measurements. Denaturant-induced equilibrium transitions were monitored by incubating the protein for 24 h at varying concentrations of GdmCl (0−5 M) in buffer (50 mM Tris-HCl, pH 7, containing 100 mM KCl, 1 mM DTT) containing either 3 mM EDTA or 3 mM $CaCl_2$. Denaturant concentrations were calculated from the refractive indices of the solutions (*27*). Samples were excited at 280 nm, and emission spectra were recorded. Buffer subtraction was done for each measurement. Protein unfolding was monitored by following changes in the intrinsic Trp emission fluorescence as a function of GdmCl concentration. The λ_{em} shifted gradually from 333 nm in 0 M GdmCl to 355 nm around 3 M GdmCl. This λ_{em} is typical for a fully solvent exposed tryptophan and is used as an indication of complete unfolding. For refolding experiments, the AIM1-g1 protein was denatured for 12 h in 6 M GdmCl in 50 mM Tris-HCl, pH 7, 100 mM KCl, 1 mM DTT at a concentration of 8 μM. Then the protein was diluted to a concentration of 0.27 μM at the indicated final GdmCl concentrations. The intrinsic Trp emission fluorescence were recorded after 4 h of incubation.

Stains-All Binding. Stains-all binding to AIM1-g1 was performed in 2 mM MOPS pH 7.2 buffer containing 30% ethylene glycol, as described earlier (*28*, *29*). Calcium-free protein solution was mixed with dye, incubated in dark for 10 min, and CD was recorded in a 1 cm path length cell from 400 to 700 nm. To study the effect of calcium on the dye-protein complex, calcium chloride solution was added, and CD spectra was recorded. The ellipticities were represented in millidegrees. The dye concentration used was 75 μM as estimated by its absorption coefficient (*28*). Protein concentration was 0.02 mg/mL. The calcium concentrations used were 0, 300 μM, 500 μM, and 1 mM.

Terbium Binding. A fresh stock solution of terbium chloride was prepared in water. The metal free protein solution (37 μg/mL) equilibrated in 50 mM Tris-HCl, pH 7.0, containing 100 mM KCl and 2 mM DTT was then

titrated by adding small aliquots of $TbCl_3$ solution (0−250 μM $TbCl_3$), allowing 15 min for equilibration after each metal addition prior to measurement. The fluorescence emission spectra were recorded from 400 to 560 nm with the excitation wavelength set at 280 nm in a F-4500 Hitachi spectrofluorimeter. The spectra were corrected with an equal amount of terbium chloride blanks.

The free Tb^{3+} concentration ($[Tb]_f$) was determined as the difference of the total ($[Tb]_{tot}$) and bound concentrations (*30*):

$$[Tb]_f = [Tb]_{tot} - [P]_{tot}\frac{F - F_{max}}{F_{max} - F_{min}} \quad (1)$$

Where $[P]_{tot}$ is the total protein concentration, F is observed Tb^{3+} emission, F_{min} is the invariant background reading in the absence of Tb^{3+}, and F_{max} is the emission when binding sites are saturated with Tb^{3+}.

The resulting binding curve was fit using the equation

$$F = (F_{max} - F_{min})\frac{[Tb]_f}{[Tb]_f + K_D} + F_{min} \quad (2)$$

Where K_D is the dissociation constant of Tb^{3+} binding to the protein.

Eq 2 was rearranged into a linear equation, and K_D was calculated from the slope of the plot $1/[Tb]_f$ versus $F_{max} - F/F - F_{min}$

^{45}Ca Overlay Method. Calcium binding to AIM1-g1 was evaluated by ^{45}Ca membrane overlay method originally described by Maruyama et al. (*31*). AIM1-g1 (50 μg) was spotted onto a PVDF membrane using a dot-blot apparatus. The membrane was equilibrated in a solution containing 10 mM imidazole-HCl, pH 6.8, 60 mM KCl, 5 mM $MgCl_2$ and then incubated for 15 min at 25 °C in the same buffer containing 1 μCi/mL of ^{45}Ca (NEN, USA) (final concentration of 2 μM $CaCl_2$). The membrane was then rinsed twice in 45% ethanol, dried, and exposed to the phosphorImager screen, and the signal was read in PhosphorImager (Fuji Bas-1800).

^{45}Ca Binding by Hummel−Dreyer Method. The binding of ^{45}Ca to AIM1-g1 protein was studied using the chromatographic method of Hummel and Dreyer (*32*). Plastic containers, tubes, and bottles were used to avoid Ca^{2+} contamination from laboratory glassware. A Sephadex G-25 column (0.7 × 40 cm) was equilibrated with 50 mM Tris buffer, pH 7.0, 100 mM KCl, 2 mM DTT containing varying amounts (0.1−20 μM) of calcium chloride solution (including ^{45}Ca). Calcium free protein solutions were equilibrated with gel-filtration buffer containing ^{45}Ca for 30 min at room temperature and applied to Sephadex G-25 column. Fractions of 0.6 mL were collected, and total radioactivity in each fraction was counted for ^{45}Ca in a Hewlett-Packard liquid scintillation counter. Bound calcium concentrations were determined from the area of the trough of these chromatograms. Klotz plot (reciprocal plot, 1/*r* vs 1/*A*) of the data collected at different free Ca^{2+} concentrations was used to estimate the binding constants (*33*).

RESULTS

Engineering and Preparation of the First $\beta\gamma$-Crystallin Domain of AIM1. We have engineered the first predicted $\beta\gamma$-crystallin domain of AIM1, designated AIM1-g1. This consists of the first two predicted $\beta\gamma$ motifs (Figure 1a), corresponding to residues 1021−1117 in the published sequence (*1*). The sequence of the domain and strategy of cloning is outlined in Figure 1b. Despite the nonconsensus sequence changes in the first motif of this domain, the recombinant protein expressed well in *E. coli* as a soluble protein. The purification was achieved by a combination of ion-exchange (Q-Sepharose, fast flow) and gel-filtration chromatography (Superdex 75 FPLC column). The purified protein was characterized by SDS−PAGE (Figure 1c) and by electrospray ionization mass spectrometry. Mass spectrometry measurements resulted in a monoisotopic mass of 10 800.4 Da, which is in agreement with the theoretical mass ($M_{r\ calc}$ = 10 807 Da).

Secondary and Tertiary Structure. To see if this domain folds properly, the native state of the recombinant protein AIM1-g1 as well as structural changes upon Ca^{2+} binding were monitored by far- and near-UV CD (Figure 2). The secondary structure shows a minimum around 218−220 nm, which indicates that the recombinant protein is in a β-sheet conformation and is properly folded (Figure 2a). In addition, there is a positive peak signal at 230−232 nm, which is known to be due to the L_a transition of Tyr with contribution from the B_b band of the indole ring of Trp (*34*−*36*). The crossover point is shifted toward blue at 196−197 nm, which could be due to the contribution via coupling of the aromatic transitions because of the proximity of these residues in the domain. Overall, the secondary structure is similar to bovine γB-crystallin conformation (*37*), including the presence of a minor hump at about 205−206 nm in the far-UV CD of both proteins. The low intensity at about 195 nm seen in the far-UV CD of AIM1-g1 is also shown by the individual domains of protein S (*21*).

The near-UV CD of AIM1-g1 is dominated by a broad band in the 255−275 nm region, indicating the CD bands for aromatic amino acids (there are three Trp, two Tyr, and two Phe); in particular, a significant contribution comes from the three Cys residues in the 250−260 nm region. In addition, there are two minima for Trp at about 288 and 294 nm (Figure 2b). We have further studied the calcium-induced changes on CD spectra. There was no significant change in near- and far-UV CD of the protein in the presence of 0.1 and 1 mM calcium. (Figure 2a,b).

Steady-State Fluorescence. We further assessed the conformation of AIM1-g1 protein by fluorescence spectroscopy. There are three Trp residues in AIM1-g1, one in the a strand of the second $\beta\gamma$ motif, and one each in the c-d loop of both $\beta\gamma$ motifs. We have looked at the fluorescence of Trp by excitation at 295 nm. The emission maximum was 333 nm (Figure 3), which indicates that Trp residues are moderately buried and are not solvent exposed. We have studied the effect of calcium on Trp fluorescence. Upon addition of calcium, there is no change in the emission spectra, indicating no conformational changes upon binding calcium (Figure 3).

AIM1-g1 Homodimerization. Since $\beta\gamma$ domains from various members of the $\beta\gamma$ superfamily are known to undergo homodimerization because of domain-domain pairing (*38*, *39*), we have studied the dimerization propensity of AIM1-g1. The native molecular mass of AIM1-g1 was determined by analytical gel filtration using a Superdex 75 size-exclusion column. To avoid covalent dimerization through disulfide

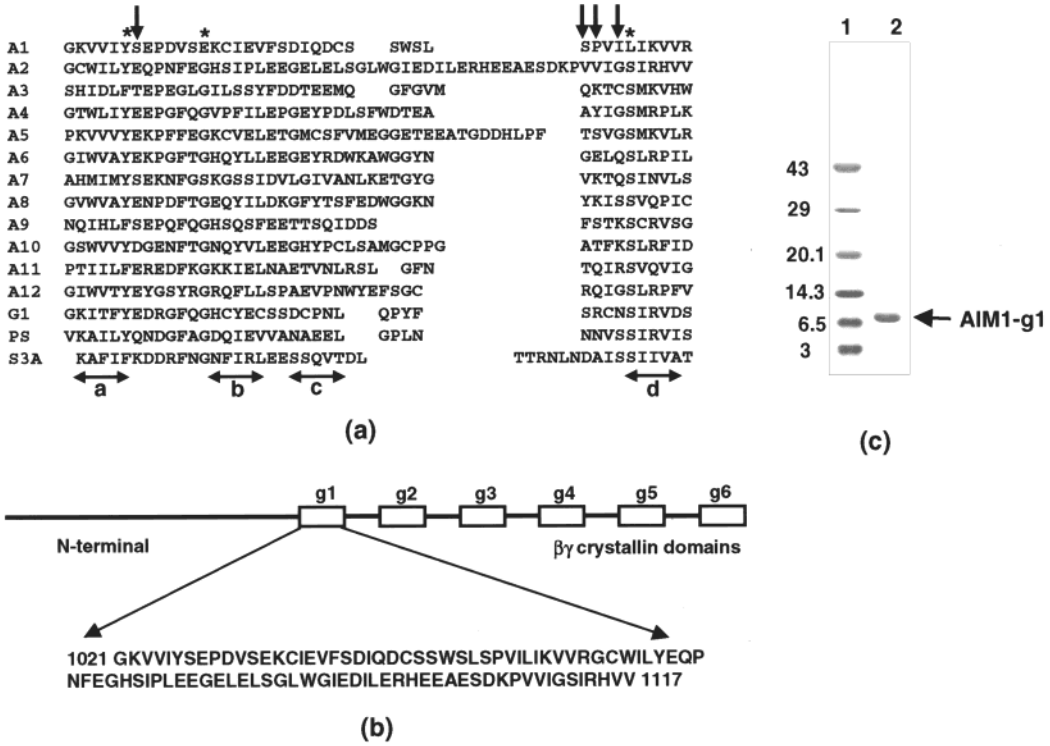

FIGURE 1: (a) Alignment of all $\beta\gamma$ motifs of AIM1. The sequences of all 12 Greek keys of AIM1 are aligned with the sequence of the Greek keys from γ-crystallin (G1), protein S (PS), and spherulin 3a (S3a). The residues, which are generally conserved in a $\beta\gamma$ crystallin fold, are marked by asterisks. Residues involved in calcium binding in protein S and spherulin 3a are indicated by solid arrows. As seen, these residues are not conserved in A1 and A2 (which form AIM1-g1) and are not likely to be involved in calcium binding. (b) The scheme for the engineering of AIM1-g1 domain. The first $\beta\gamma$ domain from 1021 to 1117 residues was selected for cloning and overexpression in the pET17b vector. The sequence of the domain region is shown. g1 to g6 represent the six $\beta\gamma$ domains of AIM1. (c) SDS−PAGE (15% acrylamide) of the purified AIM1-g1. Lane 1: molecular weight markers; lane 2: purified AIM1-g1.

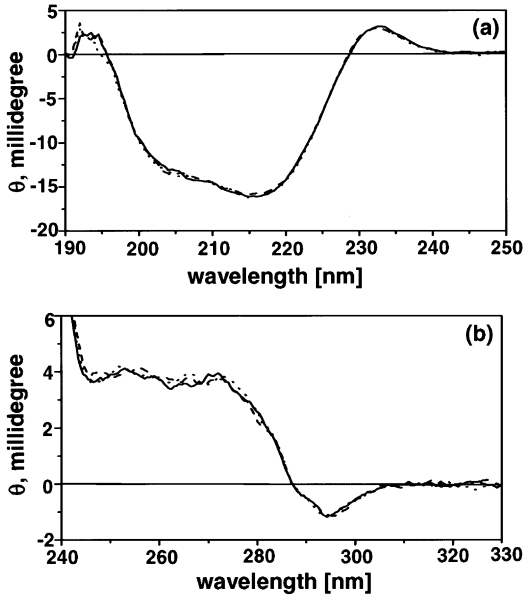

FIGURE 2: Secondary and tertiary structure of AIM1-g1. (a) Far-UV CD and (b) near-UV CD of AIM1-g1 and calcium titration. Path lengths used were 0.02 and 1 cm for far- and near-UV CD, respectively. Spectra were recorded in 50 mM Tris-HCl, pH 7 containing 100 mM KCl, 1 mM DTT. Protein concentration used was 1 mg/mL for far-UV CD and 0.4 mg/mL for near-UV CD. The ellipticity values are represented in millidegree. Calcium added was 0.1 mM calcium (dashed line) and 1 mM calcium (dotted line).

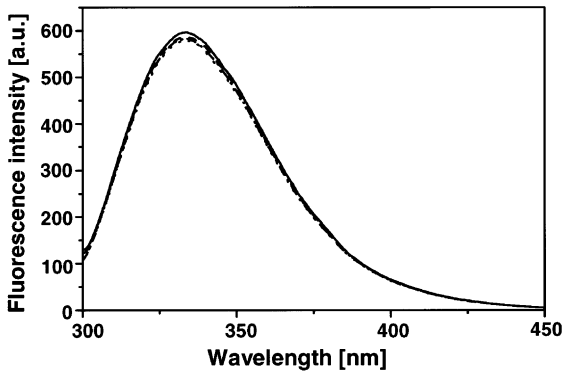

FIGURE 3: Steady-state fluorescence of AIM1-g1. Spectra were recorded in 50 mM Tris-HCl, pH 7.0 containing 100 mM KCl, 1 mM DTT. Excitation wavelength was 295 nm. Calcium was added to the protein solution, mixed, and incubated for 5 min, and the spectra were recorded in the correct spectrum mode of the instrument. The spectra were corrected by subtracting the buffer blank recorded in the same way. Calcium added was no calcium (solid line), 100 μM (dashed line), and 1 mM (dotted line).

formation, the chromatography was performed in the presence of 3 mM DTT. Under these conditions, the apparent size of AIM1-g1 was found to be 21 kDa (Figure 4), equivalent to a two-domain γB-crystallin monomer, suggesting that this domain forms homodimers. The presence of calcium (1−5 mM $CaCl_2$) has no apparent effect on dimer formation. Dimerization of single domains of γB- and γS-crystallins are not seen in dilute solutions (~1 mg/mL), although 2-fold domain pairing of identical domains of these crystallins has been observed at the high protein concentration of crystal lattices (*40*−*42*). However, the N-terminal domain of βB2-crystallin exists as dimer in solution at a concentration above 50 μg/mL (*38*). To see if dimerization

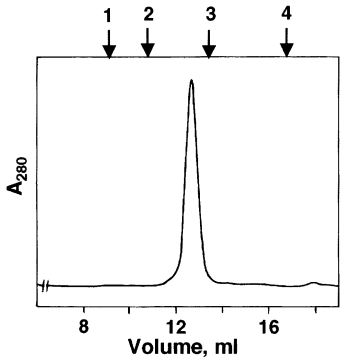

FIGURE 4: Homodimerization of AIM1-g1. Gel filtration was performed on a Superdex 75 (HR 10/30) size-exclusion column (Pharmacia-Amersham) in 50 mM Tris-HCl, pH 7.2 containing 100 mM NaCl, 1 mM EDTA, and 3 mM DTT. Flow rate was 0.5 mL per min. The molecular mass standards used were (1) albumin (66 kDa), (2) ovalbumin (45 kDa), (3) RNaseA (14 kDa), and (4) aprotinin (6.5 kDa). The single peak shown corresponds to the dimer molecular mass of 21 kDa of AIM1-g1.

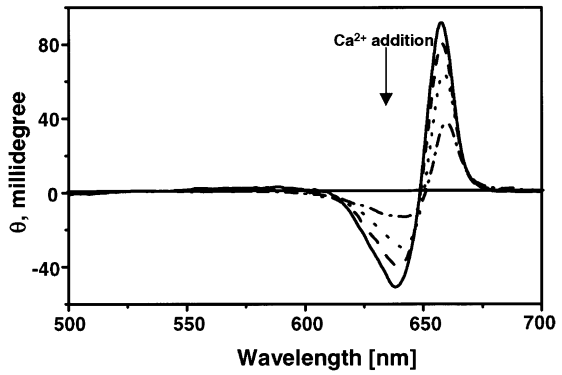

FIGURE 5: Stains-all binding to AIM1-g1. The experiments were performed in 2 mM MOPS, pH 7.2, containing 30% ethylene glycol. CD spectra were recorded in 1 cm path length cuvette, and data are represented in millidegree. The dye concentration used was 75 μM. Protein concentration was 0.02 mg/mL. The calcium concentrations used were 0 (solid), 300 μM (dotted), 500 μM (dashed), and 1 mM (dot−dashed).

of AIM1-g1 is concentration dependent, we performed Superdex 75 gel-filtration chromatography using various dilutions of AIM1-g1 protein (40 μg/mL to 1.5 mg/mL). We have observed that the self-domain pairing of AIM1-g1 is not concentration dependent and that the protein exists as a dimer even in dilute solution, as low as 40 μg/mL. This is consistent with the prediction that the domains of AIM1 associate in pairs with domain-domain interactions similar to those of βB2- and γB-crystallins (*1*, *9*). The above results suggest that the variant $\beta\gamma$ domain, AIM1-g1, adopts a typical $\beta\gamma$ domain-like conformation.

Stains-All Binding. Calcium binding to AIM1-g1 was evaluated by calcium mimic, Stains-all, a carbocyanine dye. This dye has been used to probe calcium binding in a number of calcium-binding proteins (*26*, *28*, *29*, *43*, *44*). The dye binds the recombinant protein AIM1-g1 and induces a strong J band at 660 nm (Figure 5) suggesting that it binds calcium. The intensity of the CD band is decreased upon the addition of calcium ions (Figure 5), as expected for a calcium mimic agent. Other proteins of the superfamily, namely βH- and γ-crystallins, also induce the J band of the dye indicating the similarity in the microenvironment of the dye-binding site, in keeping with the secondary structure - Stains-all

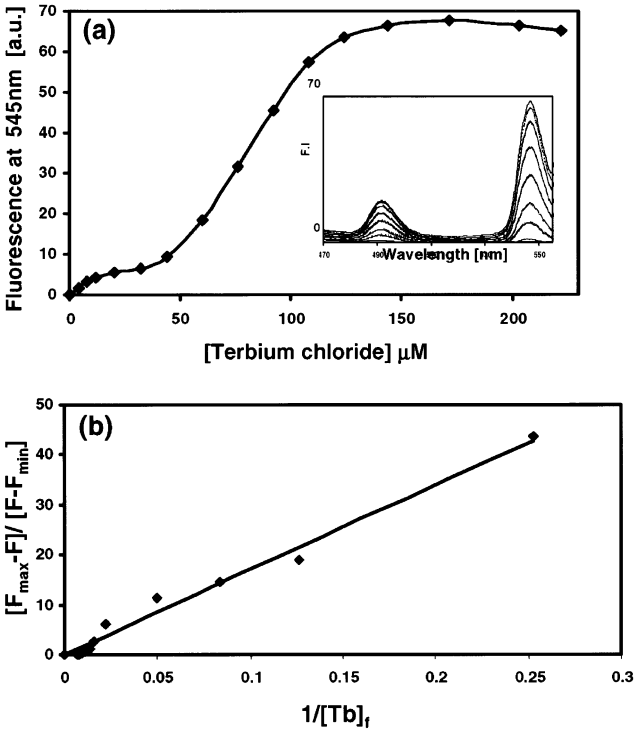

FIGURE 6: Terbium ion binding to AIM1-g1. (a) Titration of AIM1-g1 with Tb^{3+} (0−250 μM) monitored from the fluorescence emission at 545 nm. Buffer: 50 mM Tris-HCl, pH 7, 100 mM KCl, 2 mM DTT. Protein concentration was 37 μg/mL. Inset represents the spectra from 470 to 560 nm. (b) Plot of $1/[Tb]_f$ vs $F_{max} - F/ F - F_{min}$ for terbium binding to AIM1-g1.

reports on protein conformation (*29*). On the basis of the ellipticity of the induced J band, we found that the affinity of calcium to this protein is more than the affinity of bovine lens γB-crystallin using equimolar concentrations of protein (data not shown).

Terbium Binding and Fluorescence Resonance Energy Transfer (FRET). We have further probed calcium binding using another calcium probe, terbium, by FRET. Terbium is known to bind the calcium-binding sites and induce luminescence at 545 nm via energy transfer from Trp (*45*). Figure 6a shows that Tb^{3+} binds AIM1-g1 and induces luminescence at 545 nm (Figure 6a, inset). The apparent binding constant calculated for Tb^{3+} binding to AIM1-g1 is about 170 μM (Figure 6b). The terbium binding K_D of AIM1-g1 is approximately 1.7 times stronger than the K_D of Tb^{3+} to a two-domain member of the $\beta\gamma$-crystallin superfamily, bovine lens γ-crystallin, whose K_D is ∼300 μM (*26*).

^{45}Ca Binding. We have performed calcium binding by direct ^{45}Ca binding using the membrane overlay (*31*) as well as by the gel-filtration method (*32*). The calcium overlay method has been widely used to ascertain the cation binding to calcium-binding proteins. AIM1-g1 binds calcium as shown by the spot on the PVDF membrane in Figure 7a. The positive (synthesized 34 residues peptide corresponding to the fourth EF-hand of neuronal calcium sensor-1, a calcium-binding protein) and negative controls (bovine serum albumin) exhibit the respective anticipated results. We have also performed the ^{45}Ca binding by the gel-filtration method (*32*). The chromatogram in Figure 7b represents the elution profile using 1 μM calcium chloride solution containing ^{45}Ca. As seen in Figure 7b, calcium binds to the protein but elutes

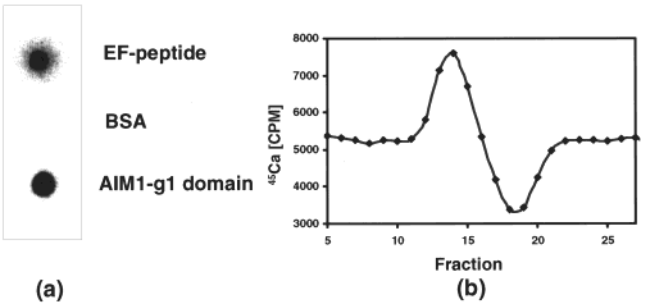

FIGURE 7: ^{45}Ca binding to AIM1-g1: (a) by membrane overlay method. The protein (50 μg) was spotted on a PVDF membrane using a dot-blot apparatus, and the membrane was incubated in the imidazole buffer containing ^{45}Ca (1 μCi/mL) as described in the Experimental Procedures. The positive control (100 μg) was an EF-hand peptide (site 4) of neuronal calcium sensor-1, and negative control was bovine serum albumin (100 μg); (b) by gel filtration: protein was prepared in calcium free buffer and Hummel−Dreyer chromatography was performed in 50 mM Tris-HCl, pH 7.0, 100 mM KCl, 2 mM DTT containing varying amounts (0.1−20 μM) of calcium chloride solution (including ^{45}Ca). Figure 7b represents an elution profile of the protein in above buffer containing 1 μM $CaCl_2$ for the measurement of bound ^{45}Ca.

Table 1: Comparison of Dissociation Constant of Calcium Binding to AIM1-g1 with Other Members of the $\beta\gamma$ Crystallin Superfamily

protein	K_D (μM)	ref
AIM1-g1	30	this paper
protein S	27, 76	*12*
spherulin 3a	9, 200	*55*
γ-crystallin	90	*26*
βH-crystallin	300	*25*

without a plateau, indicating a slow binding equilibria (*46*). The peak indicates the elution of the calcium bound protein, while the trough represents the depletion that resulted from the bound ligand, which was carried ahead with the protein. Several runs ranging from 0.1−20 μM $CaCl_2$ (including ^{45}Ca) concentrations were performed, and bound calcium concentrations were determined from the area of the trough of these chromatograms. A reciprocal plot (*33*) of the data reveals an apparent dissociation constant, K_D of about 30 μM (Table 1).

GdmCl-Induced Unfolding of AIM1-g1. β- and γ-crystallins are highly stable proteins. We have, therefore, determined the conformational stability of AIM1-g1 by GdmCl dependent equilibrium transitions. The protein was completely unfolded in about 3 M GdmCl as monitored by intrinsic Trp emission fluorescence. Figure 8 shows the fraction of native molecules as a function of GdmCl concentration. The GdmCl induced equilibrium unfolding transitions are fully reversible with a transition midpoint, $C_{1/2\ [GdmCl]}$, of 1.8 M. This value is at par with γS-crystallin and its individual domains (*47*) indicating similar stabilities (Table 2). Since calcium is known to elevate the stability of protein S and spherulin 3a significantly (*48*, *49*), we wanted to see if calcium binding influences the stability of AIM1-g1 by studying the effect of calcium on GdmCl-induced unfolding. The unfolding of AIM1-g1 in the presence (3 mM $CaCl_2$) and the absence of Ca^{2+} at different concentrations of denaturant revealed that the presence of Ca^{2+} does not affect protein stability significantly. Since calcium binding has no influence on the unfolding profile of AIM1-g1, in Figure 8, only the data of

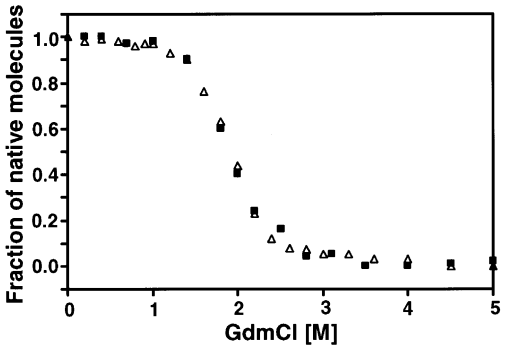

FIGURE 8: GdmCl-induced equilibrium transitions of AIM1-g1. Equilibrium unfolding transitions (open symbols) and refolding transitions (filled symbols) of AIM1-g1, monitored by following changes in the intrinsic Trp emission fluorescence as a function of GdmCl concentration (0−5 M). Excitation wavelength was 280 nm. The buffer was 50 mM Tris-HCl, pH 7, containing 100 mM KCl and 1 mM DTT.

Table 2: Midpoint of GdmCl-Induced Equilibrium Transitions ($C_{1/2,GdmCl}$) of AIM1-g1 Unfolding and Comparison with γS-Crystallin and Its Domains

protein	$C_{1/2,\ GdmCl}$ (M)	ref
AIM1-g1	1.8	this paper
human γS-crystallin	2.6	*47*
human γS-C terminal domain	2.5	*47*
human γS-N terminal domain	1.9	*47*

calcium-free protein are shown. We have seen similar behavior of calcium on the GdmCl-induced unfolding of bovine βH-crystallin (oligomeric β-crystallin) and recombinant βB2- and γB-crystallins.[2]

DISCUSSION

The structural analysis of the $\beta\gamma$-crystallin superfamily began with the X-ray structure of bovine lens γII-crystallin (now called γB) (*5*, *6*). This revealed one of the most highly symmetrical proteins known, with a characteristic 4-fold repeat of a Greek key type structural motif. This motif includes an unusual folded hairpin structure that requires the presence of several key residues. These residues constitute a sequence signature that has been used to predict the presence of similar domains in other proteins. This was first noticed in the related βB2-crystallin and later in several proteins from prokaryotes as well as from eukaryotes (*9*, *11*). To date, the most complex predicted member of the superfamily found is AIM1, a large protein whose expression has been related to melanoma suppression (*1*). The gene encoding AIM1 includes a region that resembles the concatenation of three β-crystallin genes, and its amino acid sequence contains multiple copies of the $\beta\gamma$ signature.

Recent structure determinations have shown that proteins that are no more than distantly related to the $\beta\gamma$ superfamily are able to form domains with similar arrangement of β-strands, suggesting that perfect conservation of the motif signature is not necessary to allow correct folding (*17*−*19*). However, the sequence changes in the first motif of AIM1, particularly the substitution of Glu for Gly at position 13 and Leu for Ser at 34 (Figure 1a), would seriously affect the familiar folded hairpin structure.

[2] Rajini, B., and Sharma, Y., unpublished results.

To provide more evidence for the predicted structure, we have prepared a recombinant protein for this domain, designated AIM1-g1. This one-domain protein is soluble and expresses well in *E. coli*. The secondary structure of the recombinant AIM1-g1 is predominantly a β-sheet, and the far-UV CD spectrum has the chain conformational characteristics of bovine lens γB-crystallin, except for minor variations. The hump in the CD signal at 204−206 nm seen in various γ-crystallins is also seen in the far-UV CD of AIM1-g1 (*37*). Other characteristics such as the emission maximum (333 nm) are close to that shown by bovine lens γIV-crystallin (334 nm) indicating that the AIM1-g1 domain largely resembles the γ-crystallin conformation. However, variations between γ-crystallin and AIM1-g1 are seen, such as a positive signal at about 232 nm in the far-UV CD of AIM1-g1, which is attributed to the contributions from aromatic residues (about 10% of residues are aromatic in this protein domain) largely from the L_a transition of Tyr; and the intensity of the 194 nm positive peak is considerably low in case of AIM1-g1. The low intensity of the positive peak is also seen in the case of individual domains of protein S (*21*).

Another part of the prediction for AIM1 structure is that its domains should behave like those of βB2- and γB-crystallins in terms of interdomain interactions (*1*). In both classes of crystallins, the repeated $\beta\gamma$ motifs can be classified as types A and B, so that each two-domain crystallin monomer has the motif pattern ABAB. The B-type motifs, which are generally the most highly conserved, include a small hydrophobic surface patch of two residues on the center of the β-sheet that makes up one side of the wedge-shaped β-sandwich, and two B-type motifs interact through their symmetrically related patches (*6*, *50*, *51*). In the B-type motif of AIM1-g1 (A2 in Figure 1a), the equivalent residues are Ile at position 4 and Pro at position 17. These are hydrophobic and could support the formation of a patch, although the presence of Pro would be expected to introduce some distortion in the b strand of the second motif. In spherulin 3a, a larger patch involving four hydrophobic side chains is used for dimerization (*8*). The equivalent residues in the second motif of AIM1-g1 are Ile at position 4, Phe at position 11, Ser at position 15, and Arg at position 53. The presence of Ser and Arg in this group makes it unlikely that AIM1-g1 adopts the spherulin mode of dimerization. Another complication in predicting dimerization is that dimer formation for isolated recombinant domains of $\beta\gamma$ superfamily members, at least in crystal structures, seems to be affected by the presence or absence of N- or C-terminal extensions in the recombinant protein (*8*, *21*, *38*, *41*, *52*−*54*). In view of this, we were very interested to see how AIM1-g1 behaves in solution.

The results show that AIM1-g1 homodimerizes in solution with no observable trace of monomer under the conditions tested. This suggests that the $\beta\gamma$ domains of AIM1 do associate in a crystallin-like manner. Despite the variant sequence, this domain apparently folds into a typical $\beta\gamma$ motif as revealed by our spectroscopic studies and its stability is comparable ($C_{1/2\ [GdmCl]}$ is 1.8 M) to γS-crystallin domains (Table 2). The precise nature of the interdomain contacts as well as domain topology will require more detailed structural analysis.

AIM1 Is a Calcium-Binding Protein. Our results show that AIM1 is a calcium-binding protein. We have probed the calcium-binding properties of AIM1-g1 by both direct (^{45}Ca binding to protein) and indirect methods using calcium probes (terbium and Stains-all binding). The affinity of calcium to AIM1-g1 (30 μM) is comparable to that of spherulin 3a and protein S but more than bovine γ-crystallin (containing all five γ-crystallins) and βH-crystallin (oligomeric form of β-crystallin) (Table 1). Calcium binding does not induce conformational changes in AIM1-g1, which is in agreement with the results on γ-crystallin (*26*) and on the N-terminal domain of protein S (*21*). Calcium binding to AIM1-g1 does not bring any change in protein stability as monitored by GdmCl induced unfolding. This behavior is similar to lens proteins, βB2-, and γB-crystallins. However, in case of microbial crystallin members, protein S and spherulin 3a, calcium binding increases the stability severalfold (*48*, *55*). These results suggest that there might be structural differences in the mode of calcium binding between these members.

Calcium-binding sites in members of the $\beta\gamma$ superfamily have been experimentally determined by structural analyses of the microbial proteins, spherulin 3a, and protein S (*8*, *20*, *22*, *48*). In these proteins, each $\beta\gamma$ motif contains a D/NXXS sequence element at the C-terminal end of the strand c-d loop, and the elements in two motifs combine to form two symmetrical calcium-binding sites (*8*). In AIM1-g1, the equivalent sequences in the two $\beta\gamma$ motifs are SPVI and VVIG (Figure 1a), so that out of four side chain positions needed for coordination, only one is polar. However, AIM1-g1 contains another sequence element that could contribute to binding a cation. This is the extended c-d loop of the second motif of AIM1-g1 that contains a markedly acidic stretch of residues with the sequence EDILERHEEAESD (Figure 1a). It is likely that this region would play a key role in building a negatively charged environment to bind positively charged calcium ions. Binding sites could be located in regions generally similar to those seen in spherulin 3a and protein S but stabilized specifically at either end of the acidic c-d loop region. It will be of great interest to define this binding more precisely by detailed structural analyses. Topologically, $\beta\gamma$ domain has some superficial structural similarities with the C2 domain, a calcium-binding motif of protein kinase C present in many proteins (*56*). This is also a predominantly β-sheet structure in which calcium binds at the tip of a compact β-sandwich but induces no changes in protein conformation (*57*).

In conclusion, our results show that despite variations in amino acids at a conserved position, or the presence of an unusually long c-d loop, AIM1-g1 folds such as a $\beta\gamma$ domain, undergoes dimerization and binds calcium. The structural features required for adopting a $\beta\gamma$-fold with its characteristics such as domain-domain interaction and calcium binding are not yet completely understood, and more detailed studies are required. Calcium binding could have relevance for the functional role of AIM1 in normal cells and (potentially) in tumor suppression. Indeed, defects in calcium homeostasis have been reported in several cases of malignant melanoma (*58*−*60*). It will be interesting to study the properties of other domains of AIM1, as well as the intact protein, and the effect of the long, noncrystallin-like N-terminal domain on protein assembly.

ACKNOWLEDGMENT

Thanks to Dr. Orvall Bateman of Birkbeck College, London for reagents and protocols. We thank Drs. Jeff Trent and Paul Meltzer of NHGRI for making available to us the original cDNA clones of AIM1.

REFERENCES

1. Ray, M. E., Wistow, G., Su, Y. A., Meltzer, P. S., and Trent, J. M. (1997) *Proc. Natl. Acad. Sci. U.S.A. 94*, 3229−3234.
2. Teichmann, U., Ray, M. E., Ellison, J., Graham, C., Wistow, G., Meltzer, P. S., Trent, J. M., and Pavan, W. J. (1998) *Mamm. Genome 9*, 715−720.
3. Trent, J. M., Stanbridge, E. J., McBridge, H. L., Meese, E. U., Casey, G., Araujo, D. E., Witkowski, C. M., and Nagle, R. B. (1990) *Science 247*, 568−571.
4. Wistow, G. (1995) *Molecular Biology Intelligence Series*: *Molecular Biology and Evolution of Crystallins: Gene Recruitment and Multifunctional Proteins in the Eye Lens*, R. G. Landes Company, Austin, TX.
5. Blundell, T., Lindley, P., Miller, L., Moss, D., Slingsby, C., Tickle, I., Turnell, B., and Wistow, G. (1981) *Nature 289*, 771−777.
6. Wistow, G., Turnell, B., Summers, L., Slingsby, C., Moss, D., Miller, L., Lindley, P., and Blundell, T. (1983) *J. Mol. Biol. 170*, 175−202.
7. Wistow, G., Summers, L., and Blundell, T. (1985) *Nature 315*, 771−773.
8. Clout, N. J., Kretschmar, M., Jaenicke, R., and Slingsby, C. (2001) *Structure 9*, 115−124.
9. Jaenicke, R., and Slingsby, C. (2001) *Crit. Rev. Biochem. Mol. Biol. 36*, 435−499.
10. Wistow, G., and Piatigorsky, J. (1988) *Annu. Rev. Biochem. 57*, 479−504.
11. Wistow, G., Jaworski, C., and Rao, P. V. (1995) *Exp. Eye Res. 61*, 637−639.
12. Teintze, M., Inouye, S., and Inouye, M. (1988) *J. Biol. Chem. 263*, 1199−1203.
13. Ogawa, M., Takabatake, T., Takahashi, T. C., and Takeshima, K. (1997) *Dev. Genes Evol. 206*, 417−424.
14. Ogawa, M., Takahashi, T. C., Takabatake, T., and Takeshima, K. (1998) *Dev. Growth Differ. 40*, 465−473.
15. Chan, C. W., Saimi, Y., and Kung, C. (1999) *Gene 231*, 21−32.
16. Wistow, G. (1990) *J. Mol. Evol. 30*, 140−145.
17. Clout, N. J., Slingsby, C., and Wistow, G. J. (1997) *Nature Struct. Biol. 4*, 685.
18. Antuch, W., Guntert, P., and Wuthrich, K. (1996) *Nature Struct. Biol. 3*, 662−665.
19. Ohno, A., Tate, S.-I., Sreeram, S. S., Hiraga, K., Swindells, M. B., Oda, K., and Kainosho, M. (1998) *J. Mol. Biol. 282*, 421−433.
20. Bagby, S., Harvey, T. S., Eagle, S. G., Inouye, S., and Ikura, M. (1994) *Proc. Natl. Acad. Sci. U.S.A. 91*, 4308−4312.
21. Wenk, M., Baumgarten, R., Holak, T. A., Huber, R., Mayr, E.-M., and Jaenicke, R. (1999) *J. Mol. Biol. 288*, 1533−1545.
22. Rosinke, B., Renner, C., Mayr, E.-M., Jaenicke, R., and Holak, T. A. (1997) *J. Mol. Biol. 271*, 645−655.
23. Sharma, Y., Rao, C. M., Narasu, M. L., Rao, S. C., Somasundaram, T., Gopalakrishna, A., and Balasubramanian, D. (1989) *J. Biol. Chem. 264*, 12794−12799.
24. Balasubramanian, D., and Sharma, Y. (1991) in *Novel Calcium Binding Proteins—Fundamentals and Clinical Implications* (Heizmann, C. W., Ed.) pp 361−374, Springer-Verlag, Duesseldorf, Germany.
25. Sharma, Y., and Balasubramanian, D. (1996) *Ophthalmic Res. 28-(S)*, 44−47.
26. Rajini, B., Shridas, P., Sundari, C. S., Muralidhar, D., Chandani, S., Thomas, F., and Sharma, Y. (2001) *J. Biol. Chem. 276*, 38464−38471.
27. Pace, N. C. (1986) *Methods Enzymol. 131*, 266−280.
28. Caday, C. G., and Steiner, R. F. (1985) *J. Biol. Chem. 260*, 5985−5990.
29. Sharma, Y., Rao, C. M., Rao, S. C., Somasundaram, T., Gopalakrishna, A., and Balasubramanian, D. (1989) *J. Biol. Chem. 264*, 20923−20927.
30. Drake, S. K., and Falke, J. J. (1996) *Biochemistry 35*, 1753−1760.
31. Maruyama, K., Mikawa, T., and Ebashi, S. (1984) *J. Biochem. (Tokyo) 95*, 511−519.
32. Hummel, J. P., and Dreyer, W. J. (1962) *Biochim. Biophys. Acta 63*, 530−532.
33. Klotz, I. M. (1948) *J. Am. Chem. Soc. 70*, 939−944.
34. Day, L. A. (1973) *Biochemistry 12*, 5329−5339.
35. Woody, R. W. (1978) *Biopolymers 17*, 1451−1467.
36. Sreerama, N., Manning, M. C., Powers, M. E., Zhang, J. X., Goldenberg, D. P., and Woody, R. W. (1999) *Biochemistry 38*, 10814−10822.
37. Mandal, K., Chakrabarti, B., Thomson, J., and Siezen, R. J. (1987) *J. Biol. Chem. 262*, 8096−8102.
38. Wieligmann, K., Mayr, E.-M., and Jaenicke, R. (1999) *J. Mol. Biol. 286*, 989−994.
39. Kretschmar, M., Mayr, E.-M., and Jaenicke, R. (1999) *Biol. Chem. 380*, 89−94.
40. Norledge, B. V., Mayr, E.-M., Glockshuber, R., Bateman, O. A., Slingsby, C., Jaenicke, R., and Driessen, H. P. C. (1996) *Nature Struct. Biol. 3*, 267−274.
41. Basak, A. K., Kroone, R. C., Lubsen, N. H., Naylor, C. E., Jaenicke, R., and Slingsby C. (1998) *Protein Eng. 11*, 337−344.
42. Palme, S., Jaenicke, R., and Slingsby, C. (1998) *J. Mol. Biol. 279*, 1053−1059.
43. Caday, C. G., Lambooy, P. K., and Steiner, R. F. (1986) *Biopolymers 25*, 1579−1595.
44. Sharma, Y., Chandani, S., Sukhaswami, M. B., Uma, L., Balasubramanian, D., and Fairwell, T. (1997) *Eur. J. Biochem. 243*, 42−48.
45. Horrocks, W. D., Jr. (1993) *Methods Enzymol. 226*, 495−538.
46. Ackers, G. K. (1973) *Methods Enzymol. 27*, 441−455.
47. Wenk, M., Herbst, R., Hoeger, D., Kretschmar, M., Lubsen, N. H., and Jaenicke, R. (2000) *Biophys. Chem. 86*, 95−108.
48. Wenk, M., and Mayr, E.-M. (1998) *Eur. J. Biochem. 255*, 604−610.
49. Kretschmar, M., and Jaenicke, R. (1999) *J. Mol. Biol. 291*, 1147−1153.
50. Bax, B., Lapatto, R., Nalini, V., Driessen, H., Lindley, P. F., Mahadevan, D., Blundell, T. L., and Slingsby, C. (1990) *Nature 347*, 776−780.
51. Lapatto, R., Nalini, V., Bax, B., Driessen, H., Lindley, P. F., Blundell, T. L., and Slingsby, C. (1991) *J. Mol. Biol. 222*, 1067−1083.
52. Clout, N. J., Basak, A., Wieligmann, K., Bateman, O. A., Jaenicke, R., and Slingsby, C. (2000) *J. Mol. Biol. 304*, 253−257.
53. Bateman, O. A., Lubsen, N. H., and Slingsby, C. (2001) *Exp. Eye Res. 73*, 321−331.
54. Purkiss, A. G., Bateman, O. A., Goodfellow, J. M., Lubsen, N. H., and Slingsby, C. (2002) *J. Biol. Chem. 277*, 4199−4205.
55. Kretschmar, M., Mayr, E.-M., and Jaenicke, R. (1999) *J. Mol. Biol. 289*, 701−705.
56. Shao, X., Fernandez, I., Sudhof, T. C., and Rizo, J. (1998) *Biochemistry 37*, 16106−16115.
57. Sutton, R. B., Davletov, B. A., Berghuis, A. M., Sudhof, T. C., and Sprang, S. R. (1995) *Cell 80*, 929−938.
58. Levy, I., and Feun, L. (1990) *Am. J. Clin. Oncol. 13*, 524−526.
59. des Grottes, J. M., Dumon, J. C., and Body, J. J. (2001) *Melanoma Res. 11*, 477−482.
60. Kageshita, T., Matsui, T., Hirai, S., Fukuda, Y., and Ono, T. (1999) *Melanoma Res. 9*, 69−73.

BI027384L